Camera Image Quality Assessment without Reference Information

Lijuan Tang*†, Hong Lu‡, Ke Gu§, and Jiansheng Qian†
*School of Information and Electronic Engineering, Jiangsu Vocational College of Business, China
†School of Information and Electronic Engineering, China University of Mining and Technology, China
‡School of Automation, Nanjing Institute of Technology, Nanjing, 211167, China
§School of Computer Science and Engineering, Nanyang Technological University, Singapore

***Abstract*—Blur plays an important role in the perception of camera image quality. It causes attenuation of high frequency information and accordingly changes the image energy. Recent researches in quaternion singular value decomposition show that the singular values and singular vectors of the quaternion can capture the distortion of color images, and thus singular values can be used to measure the extent of blur. Based on this, a novel training-free blind quality assessment method considering the integral color information and singular values of the distorted image is proposed for evaluating the sharpness of camera image. The blurred camera image is first converted to LAB color space and divided into blocks. Then pure quaternion is utilized to represent pixels of the blurred camera image and the energy and variance of every block are obtained. The sharpness score of blurred camera image is defined as the variance-normalized energy over a set of selected high variance blocks, which is obtained by normalizing the total block energy using the sum of block variances. Results confirm the superiority of the proposed blind algorithm in assessing camera images.**[1]

I. Introduction

With the rapid development of multimedia technology and Internet business, visual information has played an important role in human daily lives. But images are oftentimes degraded by different kinds and levels of distortions in compression [1], [2], enhancement [3], [4] and more. So it is urgent to develop effective and efficiency image quality assessment metric to assess the quality of the image so that it can be used for supervisory control and possibly enhancing the quality of images.

In the past decades, scientists have proposed many image quality metrics, which can be basically classified into subjective and objective quality assessment methods. Objective image quality assessment has attracted significant attention in recent years. Depending on the validity of reference images, objective image quality assessment metrics can be further divided into full reference (FR), reduced-reference (RR) and no reference (NR)/blind quality assessment methods [5]. FR IQA methods utilize the distortion-free image to evaluate the quality of distorted image, which works on the assumption that the reference image is accessible [6], [7], [8], [9].

[1]This work is kindly supported in part by National Science Foundation of China (61379143; 61305011), the national key research and development plan (2016YFC0801800), and Science and Technology Planning Project of Nantong (BK2014022). Hong Lu is the corresponding author for this paper.

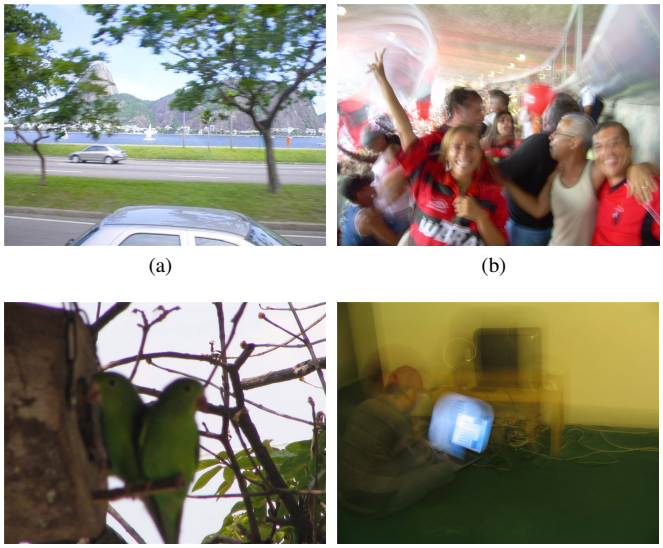

(a) (b) (c) (d)

Fig. 1. Sample realistic blur images from RBID database [21]. (a) Simple motion blur. (b) Out of focus blur. (c) Complex motion blur. (d) Other complicated distortions.

But in most scenarios, only the distorted image is available, and this type of IQA models are NR/blind IQA approaches. According to the prior knowledge of the image distortions, NR IQA models can be also separated into distortion-specific and general-purpose metrics. Typical distortion-specific NR IQA methods are devoted to blurriness/sharpness [10], [11], [12], [13], blockiness [14], [15], contrast adjustment [16], etc. In recent years, general-purpose blind metrics have been an active research field. Many NR IQA models have been proposed in [17], [18], [19], [20].

Although current image blur metrics are good at simulated blur distortion, they poorly perform for realistic camera image assessment, which can be found from experimental results in Section 4. Realistic camera images contain not only typical and easy to model blurring cases, but also more complex and realistic ones. Sample realistic camera images chosen from the RBID database [21] are illustrated in Fig. 1. It can be seen from the Fig. 1 that the realistic camera blur distorted images contain many categories of blur distortions. Image (a) may be classified into the simple motion class that could by fairly

(a) (b) (c) (d) (e) (f)

Fig. 2. Effect of changing singular values σ. The original image is shown in (a). The number of σ_{i} set as (b) i = 512. (c) i = 200. (d) i = 100. (e) i = 30. (f) i = 10.

(a) (b) (c) (d) (e) (f)

Fig. 3. Effect of changing $\mathbf{U}\mathbf{V}^T$ values. (a) denotes original image. The number of group $\mathbf{U}_i\mathbf{V}_i^T$ set as (b) i = 512. (c) i = 300. (d) i = 100. (e) i = 50. (f) i = 10.

considered linear caused by camera movements. Image (b) consists of complex motion blur which caused by complex motion paths. Image (c) belongs to out of focus category which caused by the whole image is out of focus. Image (d) contains complex blur distortion which may contains any other types of degradation. Hence, it is challenging to evaluate the quality of realistic blur images.

This paper concentrates on blind camera image sharpness assessment. Compared with previous works, to the best of our knowledge, our research is the first work to propose a blind sharpness of camera images on the basis of quaternion singular values decomposition which concerns the inevitable effect of color information on the sharpness assessment. Furthermore, the proposed blind quality metric for camera images sharpness assessment (BQSVD) can acquire sharpness scores highly consistent with the human visual system (HVS).

The rest of this paper is arranged as follows: Section 2 presents the theories of the related algorithms employed in this paper. The description of the proposed metric is introduced in section 3. In Section 4, thorough experiments are conducted using the RBID database [21] to verify the effectiveness of our BQSVD model with recently devised blind sharpness IQA metrics. Conclusions are drawn in Section 5.

II. Related work/Background

Objective quality assessment method can be considered as a two-step process consisting of feature extraction and feature pooling to create a scalar index as the quality score. As for the first step, features extraction plays a critical role for objective perceptual quality assessment which should effectively reflect the visual quality variations, while the second step decides the relationship among different features and the visual quality. Various transforms, such as singular value decomposition (SVD), discrete wavelet transform (DWT), discrete cosine transform (DCT), and discrete Fourier transform (DFT), are used for feature extraction. The changes in transformation coefficients measure visual quality. Taking account of frequency domain transforms, e.g. DCT or DFT, the basis images are same for all the images while the basis images for SVD are unique for each image. Hence, SVD is more advantageous for description visual signal and has been successfully applied to statistics and signal processing field [22].

SVD is one of the most famous transformation in linear algebra. Formally, the mathematical definition of SVD for an image matrix $\mathbf{W}_{m\times n}$ can be defined as

$$\mathbf{W}_{m\times n} = \mathbf{U}_{m\times m}\mathbf{S}_{m\times n}\mathbf{V}_{m\times n} \tag{1}$$

where $\mathbf{U}$ is an $m \times m$ unitary matrix; $\mathbf{V}$ is an $n \times n$ unitary matrix; $\mathbf{S}$ is a $m \times n$ rectangular diagonal matrix with non-negative real numbers on the diagonal. The diagonal entries σ_i are listed in descending order and known as the singular values of W. We can define U and V to be

$$\begin{aligned} \mathbf{U} &= [\mathbf{u}_1, \quad \mathbf{u}_2, \quad \cdots \quad \mathbf{u}_m] \\ \mathbf{V} &= [\mathbf{v}_1, \quad \mathbf{v}_2, \quad \cdots \quad \mathbf{v}_n]. \end{aligned} \tag{2}$$

The columns of U and V are orthonormal bases, known as the left singular vectors and the right singular vectors of $\mathbf{W}$, respectively. The matrix $\mathbf{U}\mathbf{v}^T$ can represent the image structure (the basis image), whereas the singular values σ_{i} are the weights assigned to these basis images [23]. To visually view the effect of singular value and singular vector on the image, we show examples in Fig. 2 and Fig. 3. It can be seen from Fig. 2 that the singular values σ_{i} are mainly related to the luminance changes in images, which can also be related to the changes in the frequency components of the image. We can observe from Fig. 3 that the first few singular vectors account

for the major image structure, whereas following account for the details in the image [23].

Singular values and singular vectors can describe features of images, which may be used for quality assessment. In 1843, Hamilton proposed the concept of quaternion [24]. Quaternion is an expansion of complex, namely hyper complex numbers. A quaternion is consisted of four parts, one real number and three imaginary numbers which can be described by

$$\mathbf{Q} = a + bi + cj + dk \tag{3}$$

where a, b, c and d are real numbers, i, j and k are the imaginary units. Due to the relations between the three imaginary parts, the multiplication of quaternions is not commutative. The multiplication rules between the three imaginary numbers are:

$$\begin{aligned} ij &= -ji = k \\ ki &= -ik = j \\ jk &= -kj = i \\ i^2 &= j^2 = k^2 = ijk = -1. \end{aligned} \tag{4}$$

There are other notations for quaternions [25]. A quaternion $\mathbf{Q}$ can be expressed as

$$\mathbf{Q} = \alpha + \beta j \tag{5}$$

where $\alpha = a + bi \in C$ and $\beta = c + di \in C$. This is known as Cayley-Dickson notation for quaternion matrix. The conjugate of a quaternion is defined as

$$\overline{\mathbf{Q}} = a - bi - cj - dk. \tag{6}$$

A pure quaternion is the case with a null real part (the first real number a = 0). Pure quaternion is widely used to represent color image, which the three imaginary parts represent the three channels of the color image. So a color image can be expressed by the pure quaternion:

$$\mathbf{Q}_{I(m,n)} = F_{R(m,n)}i + F_{G(m,n)}j + F_{B(m,n)}k \tag{7}$$

where $\mathbf{R}(m,n)$, $\mathbf{G}(m,n)$ and $\mathbf{B}(m,n)$ denotes the red, green and blue of the pixel (m,n) of the color image.

SVD is a factorization of a matrix. Hence, it can be directly applied to gray images. For a color image, one way is to directly operate SVD on one channel of the color image, and another way is through transforming the color image to extract the brightness level information before using the SVD method to deal with. Both of the two ways cannot handle the color image as a whole, neglecting the color information of the color image. However, the quaternion model can describe the color image information as a whole, according to the definition of SVD on the complex adjoint matrix, quaternion singular value decomposition (QSVD) can be utilized to evaluate the quality of color images. The QSVD of a quaternion Q can be defined as follows [26], [27]:

$$\mathbf{F}_{Q(m,n)} = \mathbf{U}_{m\times m}\mathbf{S}_{m\times n}\begin{pmatrix} \sum_r & 0 \\ 0 & 0 \end{pmatrix}\mathbf{V}^{\star}_{n\times n} \tag{8}$$

$$\begin{aligned} \mathbf{U} &= [\mathbf{u}_1, \quad \mathbf{u}_2, \quad \cdots \quad \mathbf{u}_m] \\ \mathbf{V} &= [\mathbf{v}_1, \quad \mathbf{v}_2, \quad \cdots \quad \mathbf{v}_n], \end{aligned} \tag{9}$$

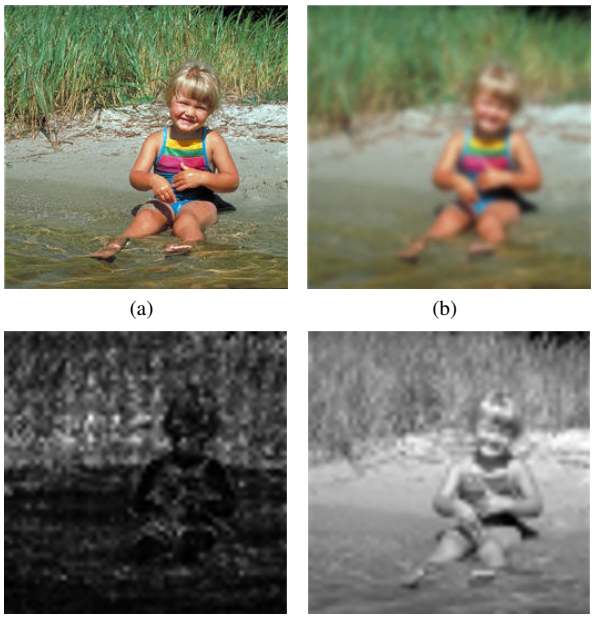

Fig. 4. (a) and (b) are the original childswimming image and the corresponding blur distortion image. (c) and (d) are the distortion maps of the gray scale SVD and QSVD of the blur distorted images, respectively.

$$\sum_r = diag(\sigma_1, \sigma_2, \cdots, \sigma_r) \tag{10}$$

where $\sum_r$ is real diagonal matrix with non-negative real numbers on the diagonal. These non-negative real numbers are the singular values of the quaternion matrix $Q(m,n)$ and r is the rank of $Q(m,n)$. V and U are the right and left singular vectors of quaternion matrix $Q(m,n)$ and elements of these two unitary matrixes are all quaternions. $*$ denotes the conjugate transpose.

To intuitional understanding the gray scale SVD that only concentrated on luminance information, and QSVD combined luminance and chrominance information into the IQA model, we give an example in Fig. 4. The subsequent formula is used to construct the distortion map [28].

$$\mathbf{D}(i) = \sqrt{\sum_{i=1}^{P}(\mathbf{S}_{dis}(i) - \mathbf{S}_{org}(i))^2} \tag{11}$$

where $\mathbf{S}_{org}$ denotes the singular values of the original block, $\mathbf{S}_{dis}$ denotes the singular values which are obtained by gray scale SVD and QSVD method of the distorted block, P is the block size. The set of distances $\mathbf{D}(i)$, when displayed in graph by mapping $\mathbf{D}(i)$ values to the range [0, 255], a gray scale image can be obtained representing distortion map.

It can be obviously seen from the figure that the gray scale SVD method, which only extracts the luminance components and discards many effective components, can not intuitionally reflect the distortion degree. However, QSVD performs better, which implies that the chrominance information should be considered when assess color image quality.

III. The Proposed Blind Quality Metric

So far, many visual quality metrics have been proposed for objective image quality assessment. They are good in simulated distortions, but poorly perform for realistic camera image assessment. Camera images have complex distortion, just as the color crosstalk effect which introduces blur with desaturation is difficult to measure [29]. In this research we deploy QSVD to measure the extent of blur in camera images. The theoretical foundation is that Frobenius norm of hyper complex matric can be used to represent the energy of color camera images, and we have a reason to believe energy change can be effectively reflect the extent of blur.

In our work, a novel hyper complex SVD-based blind camera image assessment metric is proposed. The flowchart of the proposed method is shown in Fig. 5. It consists of three main stages. In the first stage, the input blurred image is converted into LAB color space, and is represented by pure quaternion. In the second stage, two components are calculated: 1) quaternion singular values for blocks; 2) variances of blocks of the blurred camera image. Finally, effective pooling method is utilized to acquire the blur score of the input blurred camera images.

According to the previous researches, it was found that the HVS is much more sensitive to luminance changes than chrominance changes [28]. Therefore, most previous IQA methods were devised based on the mathematical modeling. Our metric considers the inevitable influence of color information on the sharpness assessment. So, in the proposed metric, the blurred camera image is first converted into widely used LAB color space [30].

Since the LAB color space is designed to approximate human vision, unlike the RGB and CMYK color space, it includes all the colors visible to the human eye and is created to serve as a device independent model. The LAB model is a three dimensional model, and the nonlinear relations for L, A and B are intended to mimic the nonlinear response of the eye. The three coordinates of LAB represents the lightness of the color (L = 0 yields black and L = 100 indicates diffuse white; specular white may be higher), its position between red/magenta and green (A, positive values indicate red while negative values indicate green), its position between yellow and blue (B, positive values indicate yellow while negative values indicate blue). There are no simple formulas for conversion between RGB values and LAB, because the RGB color model is device-dependent. Therefore, the RGB values first must be transformed to a specific absolute color space. The resulting data from the transform is device independent, allowing data to be transformed into the LAB color space.

The transformation can be defined as follows:

$$\begin{aligned} \mathbf{L} &= 116 f(Y/Y_n) - 16 \\ \mathbf{A} &= 500[f(X/X_n) - f(Y/Y_n)] \\ \mathbf{B} &= 200[f(Y/Y_n) - f(Z/Z_n)] \end{aligned} \tag{12}$$

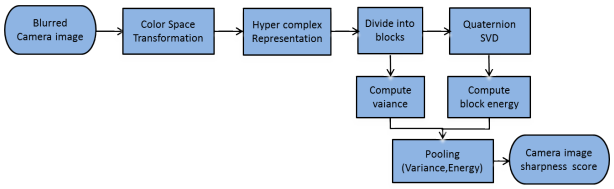

Fig. 5. Flowchart of the proposed camera image sharpness metric.

where

$$f(t) = \begin{cases} t^{1/3} & \text{if } t > (\frac{6}{29})^3 \\ \frac{1}{3}(\frac{29}{6})^2 t + \frac{4}{29} & \text{otherwise} \end{cases} \tag{13}$$

where X_n, Y_n and Z_n are the $CIEXYZ$ tristimulus values of the reference white point. Under Illuminant D65, the values are $X_n = 95.047$, $Y_n = 100.000$, $Z_n = 108.883$.

The division of the domain of the function $f(t)$ into two parts are done to prevent an infinite slope at $t = 0$. $f(t)$ was assumed to be linear below some $t = t_0$, and was assumed to match the $t^{1/3}$ part of the function at t_0 in both value and slope. In other words:

$$t_0^{1/3} = at_0 + b, \tag{14}$$

$$\frac{1}{3} t_0^{-2/3} = a. \tag{15}$$

Eq. (14) matchs in value and Eq. (15) matchs in slope. The intercept $f(0) = b$ was chosen so that $\mathbf{L}$ would be 0 for $Y = 0$, $b = 16/116 = 4/29$. The above two equations can be solved for a and t_0:

$$a = \frac{1}{3}\delta^{-2} = 7.787037\ldots \tag{16}$$

$$t_0 = \delta^3 = 0.008856\ldots \tag{17}$$

where $\delta = 6/29$ [30].

After the transformation, the pure quaternion is used to express every pixels of the transformed blurred camera image:

$$\mathbf{F}_{Q(m,n)} = F_{L(m,n)} i + F_{A(m,n)} j + F_{B(m,n)} k \tag{18}$$

where $L(m,n)$, $A(m,n)$ and $B(m,n)$ are the three channels of LAB; L denotes the luminance information; A and B for the color-opponent dimensions based on nonlinearly compressed coordinates. Frobenius norm can be utilized to represent the energy $\mathbf{E}$ of a matrix $\mathbf{A}$:

$$\mathbf{E} = \|\mathbf{A}\|_F. \tag{19}$$

Therefore, Frobenius norm of hyper complex matric $\mathbf{A}$ can be used to represent the energy of color camera images ($\mathbf{E}$). According to the definition of the hyper complex singular value decomposition, for any hyper complex matrix $\mathbf{A} \in \mathbf{H}^{M \times N}$, there exist two unitary hyper complex matrix $\mathbf{U}$ and $\mathbf{V}$,

$$\mathbf{A} = \mathbf{U} \begin{pmatrix} \sum_r & 0 \\ 0 & 0 \end{pmatrix} \mathbf{V}^\star \tag{20}$$

where $\mathbf{U} \in \mathbf{H}^{M \times M}$,$\mathbf{U} \in \mathbf{H}^{M \times M}$. Superscript $\star$ denotes conjugate transpose, $\sum_r$ is a real diagonal matrix that contains

(a) $\mathbf{E} = 46.4592$ (b) $\mathbf{E} = 46.8640$ (c) $\mathbf{E} = 53.3717$

Fig. 6. Three realistic camera images and their average energies of blocks for images with different level blur.

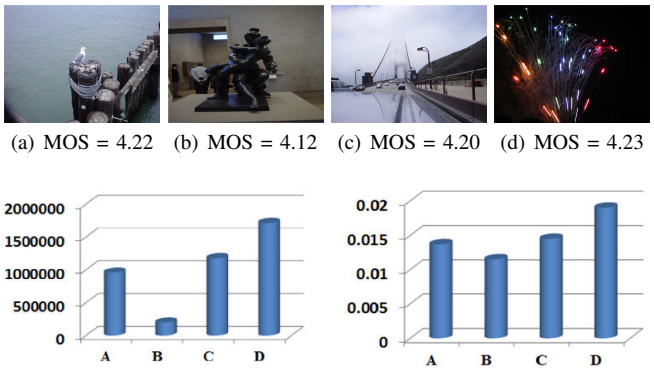

(a) MOS = 4.22 (b) MOS = 4.12 (c) MOS = 4.20 (d) MOS = 4.23

(e) Energy before normalization (f) Energy after normalization

Fig. 7. Four realistic camera images with similar MOS values together with the energy before and after normalization.

the number of r non-empty values. According to Eq. (19) and Eq. (20), the energy of color camera image can be defined as:

$$\begin{aligned}\mathbf{E} &= \|\mathbf{A}\|_F \\ &= \|\mathbf{U} \cdot \begin{pmatrix} \sum_r & 0 \\ 0 & 0 \end{pmatrix} \cdot \mathbf{V}^\star\|_F \\ &= \|\mathbf{U}\|_F \cdot \| \begin{pmatrix} \sum_r & 0 \\ 0 & 0 \end{pmatrix} \|_F \cdot \|\mathbf{V}^\star\|_F \\ &= \| \begin{pmatrix} \sum_r & 0 \\ 0 & 0 \end{pmatrix} \|_F.\end{aligned} \tag{21}$$

Since $\mathbf{U}$, $\mathbf{V}$ is unitary hyper complex matrix, their Frobenius norm equals to 1. According to Eq. (21), the energy of color camera image can be decided by the Frobenius norm of hyper complex matrix singular values. In other words, the singular values of hyper complex matrix denotes the energy feature of the color image, and it can be utilized as benchmark for evaluating the quality of color image. It serves as the theoretical basis for our proposed blind camera sharpness assessment metric.

Blur causes attenuation of high frequency information in images, and the quaternion singular values change accordingly. To have an intuitional view of the relation between quaternion singular values and blur, an example is given in Fig. 6, in which three realistic camera images with different blur scales and their energy are shown. It is can be viewed from the figure that the energy change with the degree of blur. Therefore, the energy can be used to measure the degree of sharpness with the same content. To obtain a blind sharpness metric, the influence of image content should be considered. An example shown in Figs. 7(a)-(d) has similar MOS values with similar extent of blur, but their energies differ significantly. Hence, to remove the influence of image content, the total block variances is utilized to normalized the total energy. Fig. 7(e) shows the energy of the image (a)-(d), and Fig. 7(f) shows the corresponding variance normalized energy. We can see from the Fig. 7(e) that the energy without normalization fails to predict the sharpness of image with different contents. However, when the energies are normalized by the variances, the predicted scores are similar. Hence, it can effectively evaluate the sharpness of images with different contents.

We summary the proposed BQSVD algorithm below. For a blurred RGB camera image, it is first converted to LAB color space, which is denoted by $I(x, y, z)$, $x \in 1, 2, 3, \cdots, m$, $y \in 1, 2, 3, \cdots, n$, $z \in 1, 2, 3, \cdots, k$. Next, the image is divided into blocks with equal-size non-overlap $P \times P$. The block size used in the proposed method is 8×8, since the standard block size used in the JPEG compression and many image processing applications are all 8×8 based. The pure quaternion is used to represent the three channel $\mathbf{L}$, $\mathbf{A}$ and $\mathbf{B}$. The block set is denoted by $\mathbf{B}_j$, where $j \in \{1, 2, \cdots, K\}$, $K = \times * \lfloor M = m/P \rfloor \times \lfloor N = n/P \rfloor$ and $\lfloor \cdot \rfloor$ is the floor operation. Then the variances of the blocks in $\mathbf{B}_j$ are computed and denoted by ξ_j^2. The normalized energy of the blocks are computed by

$$\mathbf{S} = \frac{\sum_{j=1}^{K} \mathbf{E}_j}{\sum_{j=1}^{K} \xi_j^2} \tag{22}$$

where $\mathbf{S}$ is the sharpness score; $\mathbf{E}_j$ and ξ_j^2 denote the energy and variance of the j^{th} block. The HVS generally inclines to judge the sharpness of an image according to the sharpest regions. In [11], the sharpness score was obtained by taking the average sharpness of 1% largest values in the sharpness map. In our proposed method, the blocks are ordered by their variances, and the $t\%$ highest variance blocks are utilized to obtain the final sharpness score as following.

$$\mathbf{S}_{BQSVD} = \frac{\sum_{j=1}^{T} \mathbf{E}_i}{\sum_{j=1}^{T} \xi_i^2} \tag{23}$$

where $T = \lfloor t\% \times K \rfloor$ denotes the number of first high variance blocks. The normalized energy based variance can effectively predict the extent blur of camera image and consistent with the subjective opinion scores.

IV. Experimental Validations

The performance of the proposed metric is evaluated on the realistic blur database (RBID) camera image quality database [21]. The images in this database are obtained for a variety of scenes, camera apertures, varying lighting conditions and exposure times. The database contains 586 images with resolutions ranging from 640×480 to 2816×2112 pixels which contains not only typical and easy to model blurring cases, but also more complex and realistic ones. The subjective qualities of the images in RBID are measured using mean opinion score with values the range from 0 to 5.

TABLE I
PERFORMANCE COMPARISON ON THE RBID DATABASE.

Metric	PLCC	SRCC	KRCC	RMSE
CPBD [10]	0.2704	0.2711	0.1820	1.2053
S3 [11]	0.4270	0.4253	0.2921	1.1320
ARISM [12]	0.1841	0.1841	0.1258	1.2305
BIBLE [13]	0.3816	0.3846	0.2611	1.1572
NIQE [17]	0.4608	0.4584	0.3089	1.1111
NFERM [20]	0.4738	0.4679	0.3183	1.1025
BQSVD (Proposed)	**0.4849**	**0.4752**	**0.3230**	**1.0949**

According to the VQEG suggestions [31], four criterions are adopted to evaluate the performance, including Spearman rank order correlation coefficient (SRCC), Kendall's rank correlation coefficient (KRCC), Pearson linear correlation coefficient (PLCC), and root mean square error (RMSE). SRCC and KRCC are used to measure the prediction monotonicity, while PLCC and RMSE are towards evaluating the prediction accuracy. Generally, a good metric produce high SRCC, KRCC and PLCC values, as well as a low RMSE value.

In this section, the performance of the proposed model is computed on the RBID database and compared with the state-of-the-art blind sharpness and quality metrics, including CPBD [10], S3 [11], ARISM [12], BIBLE [13], NIQE [17], as well as NFERM [20]. Experimental results are listed in Table II, where the best results are marked in boldface. One can see that the proposed metric produces the best results, which achieves the highest PLCC, SRCC and KRCC as well as the smallest RMSE compared with state-of-the-art competitors.

V. CONCLUSION

In this paper we have put forward a blind quality index for camera images sharpness with quaternion singular value decomposition. A comparison of our Q-SVD with popular blind sharpness measures is conducted on the RBID database. Experimental results have proved the effectiveness of the proposed blind quality measure on the RBID database. Apart form the superior performance, to our knowledge, our BQSVD technique is the first one using hypercomplex singular value decomposition towards blind image quality assessment.

REFERENCES

[1] K. Gu, S. Wang, G. Zhai, S. Ma, and W. Lin, "Screen image quality assessment incorporating structural degradation measurement," *in Proc. IEEE Int. Symp. Circuits and Syst.*, pp. 125-128, May 2015.

[2] S. Wang, K. Gu, K. Zeng, Z. Wang, and W. Lin, "Perceptual screen content image quality assessment and compression," *in Proc. IEEE Int. Conf. Image Process.*, pp. 1434-1438, Sep. 2015.

[3] K. Gu, G. Zhai, X. Yang, W. Zhang, and C. W. Chen, "Automatic contrast enhancement technology with saliency preservation," *IEEE Trans. Circuits Syst. Video Technol.*, vol. 25, no. 9, pp. 1480-1494, Sep. 2015.

[4] S. Wang, K. Gu, S. Ma, W. Lin, X. Liu, and W. Gao, "Guided image contrast enhancement based on retrieved images in cloud," *IEEE Trans. Multimedia*, vol. 18, no. 2, pp. 219-232, Feb. 2016.

[5] W. Lin and C.-C. Jay Kuo, "Perceptual visual quality metrics: A survey," *J. Vis. Commun. Image Represent.*, vol. 22, no. 4, pp. 297-312, May 2011.

[6] Z. Wang, A. C. Bovik, H. R. Sheikh, and E. P. Simoncelli, "Image quality assessment: From error visibility to structural similarity," *IEEE Trans. Image Process.*, vol. 13, no. 4, pp. 600-612, Apr. 2004.

[7] L. Zhang, L. Zhang, X. Mou, and D. Zhang, "FSIM: A feature similarity index for image quality assessment," *IEEE Trans. Image Process.*, vol. 20, no. 8, pp. 2378-2386, Aug. 2011.

[8] K. Gu, S. Wang, H. Yang, W. Lin, G. Zhai, X. Yang, and W. Zhang, "Saliency-guided quality assessment of screen content images," *IEEE Trans. Multimedia*, vol. 18, no. 6, pp. 1-13, Jun. 2016.

[9] K. Gu, S. Wang, G. Zhai, W. Lin, X. Yang, and W. Zhang, "Analysis of distortion distribution for pooling in image quality prediction," *IEEE Trans. Broadcasting*, vol. 62, no. 2, pp. 446-456, Jun. 2016.

[10] N. D. Narvekar and L. J. Karam, "A no-reference image blur metric based on the cumulative probability of blur detection (CPBD)," *IEEE Trans. Image Process.*, vol. 20, no. 9, pp. 2678-2683, Sep. 2011.

[11] C. T. Vu, T. D. Phan, and D. M. Chandler, "S3: A spectral and spatial measure of local perceived sharpness in natural images," *IEEE Trans. Image Process.*, vol. 21, no. 3, pp. 934-945, May 2012.

[12] K. Gu, G. Zhai, W. Lin, X. Yang, and W. Zhang, "No-reference image sharpness assessment in autoregressive parameter space," *IEEE Trans. Image Process.*, vol. 24, no. 10, pp. 3218-3231, Oct. 2015.

[13] L. Li, W. Lin, X. Wang, G. Yang, K. Bahrami, and A. C. Kot, "No-reference image blur assessment based on discrete orthogonal moments," *IEEE Trans. Cybernetics*, vol. 46, no. 1, pp. 39-50, 2016.

[14] S. A. Golestaneh and D. M. Chandler, "No-reference quality assessment of JPEG images via a quality relevance map," *IEEE Signal Process. Lett.*, vol. 21, no. 2, pp. 155-158, Feb. 2014.

[15] X. Min, *et. al*, "Blind quality assessment of compressed images via pseudo structural similarity," *in Proc. IEEE Int. Conf. Multimedia and Expo*, *best student paper candidate*, 2016.

[16] K. Gu, W. Lin, G. Zhai, X. Yang, W. Zhang, and C. W. Chen, "No-reference quality metric of contrast-distorted images based on information maximization," *IEEE Trans. Cybernetics*, 2017, in press.

[17] A. Mittal, R. Soundararajan, and A. C. Bovik, "Making a 'completely blind' image quality analyzer," *IEEE SPL*, vol. 22, no. 3, 2013.

[18] K. Gu, G. Zhai, W. Lin, X. Yang, and W. Zhang, "Learning a blind quality evaluation engine of screen content images," *Neurocomputing*, vol. 196, pp. 140-149, Jul. 2016.

[19] K. Gu, G. Zhai, X. Yang, and W. Zhang, "Hybrid no-reference quality metric for singly and multiply distorted images," *IEEE Trans. Broadcasting*, vol. 60, no. 3, pp. 555-567, Sept. 2014.

[20] K. Gu, G. Zhai, X. Yang, and W. Zhang, "Using free energy principle for blind image quality assessment," *IEEE Trans. Multimedia*, vol. 17, no. 1, pp. 50-63, Jan. 2015.

[21] A. Ciancio, A. L. N. T. Da Costa, E. A. da Silva, A. Said, R. Samadani, and P. Obrador, "No-reference blur assessment of digital pictures based on multifeature classifiers," *IEEE Trans. Image Process.*, vol. 20, no. 1, pp. 64-75, Jan. 2011.

[22] O. Alter, P. O. Brown, and D. Botstein, "Singular value decomposition for genome-wide expression data processing and modeling," *Proceedings of the National Academy of Sciences of the United States of America (PNAS)*, vol. 97, no. 18, pp. 10101-10106, Sep. 2000.

[23] M. Narwaria and W. Lin, "SVD-based quality metric for image and video using machine learning," *IEEE Trans. Sys., Man, and Cybernetics, Part B: Cybernetics*, vol. 42, no. 2, pp. 347-364, Apr. 2012.

[24] W. R. Hamilton, Elements of Quaternions, Longmans, Green and Company, 1866.

[25] W. R. Hamilton, Researches respecting quaternions, Trans. Roy. Irish Acad. XXI (1848) 199-296.

[26] S. J. Sangwine and N. Le Bihan, "Quaternion singular value decomposition based on bidiagonalization to a real or complex matrix using quaternion Householder transformations," *Applied Mathematics and Computation*, vol. 182, no. 1, pp. 727-738, Nov. 2006.

[27] N. Le Bihan and J. Mars, "Singular value decomposition of quaternion matrices: A new tool for vector-sensor signal processing," *Signal Process.*, vol. 84, no. 7, pp. 1177-1199, 2004.

[28] A. Shnayderman, A. Gusev, and A. M. Eskicioglu, "An SVD-based grayscale image quality measure for local and global assessment," *IEEE Trans. Image Process.*, vol. 15, no. 2, pp. 422-429, Feb. 2006.

[29] A. Kolaman and O. Yadid-Pecht, "Quaternion structural similarity: A new quality index for color images," *IEEE Trans. Image Process.*, vol. 21, no. 4, pp. 1526-1536, 2012.

[30] János Schanda, Colorimetry. Wiley-Interscience, p. 61, 2007. ISBN 978-0-470-04904-4.

[31] VQEG, "Final report from the video quality experts group on the validation of objective models of video quality assessment," Mar. 2000, http://www.vqeg.org/.